

A single-sided representation for the homogeneous Green's function, accounting for all multiples

Kees Wapenaar, Joeri Brackenhoff, Jan Thorbecke, Joost van der Neut and Evert Slob

Introduction

The homogeneous Green's function, i.e., the superposition of the causal Green's function and its time reversal, is traditionally represented by a closed boundary integral (Porter, 1970). This integral representation finds applications in holographic imaging (Esmersoy and Oristaglio, 1988), seismic interferometry (Wapenaar et al., 2005) and time-reversal acoustics (Fink, 1997). In principle these methods account for all multiples, but only when the medium is accessible from all sides. Here we discuss a single-sided representation of the homogeneous Green's function, which also accounts for all multiples, but which can be used when the medium is accessible from one side only. We indicate the application of this representation for seismic imaging, accounting for internal multiple scattering.

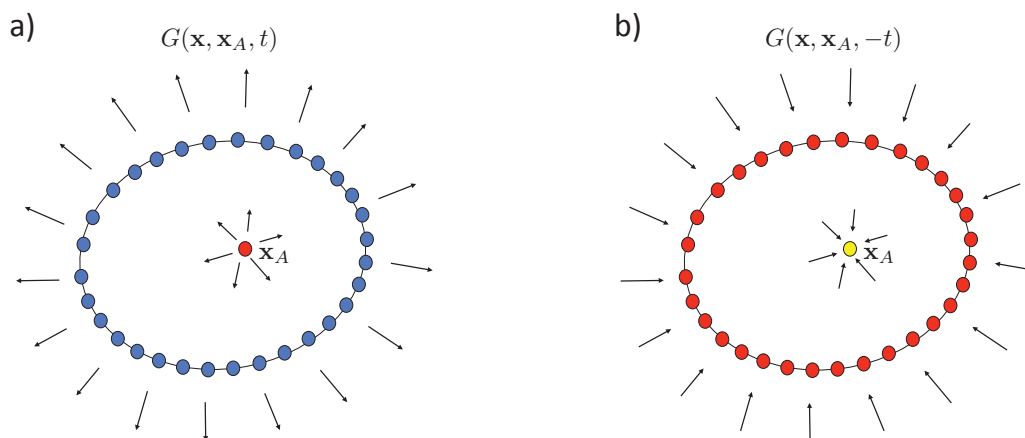


Figure 1 Principle of time-reversal acoustics. (a) Response to a source at \mathbf{x}_A at $t = 0$, observed by receivers at a closed boundary. (b) Emission of the time-reversed response by sources at the closed boundary. The field focuses at \mathbf{x}_A at $t = 0$. Subsequently the focal point \mathbf{x}_A acts as a virtual source.

Review of time-reversal acoustics

Before we introduce the single-sided representation, we briefly review the principle of time-reversal acoustics (Fink, 1997). Figure 1a illustrates the response to a source at \mathbf{x}_A at $t = 0$ in an arbitrary inhomogeneous medium. It is denoted by the Green's function $G(\mathbf{x}, \mathbf{x}_A, t)$. This response is recorded by receivers on a boundary enclosing the source. In a time-reversal experiment, the time-reversed response $G(\mathbf{x}, \mathbf{x}_A, -t)$ is emitted into the medium by sources at the positions of the original receivers (Figure 1b). Assuming the medium is lossless the field propagates back to \mathbf{x}_A , where it focuses at $t = 0$. Because there is no sink to absorb the energy of the focused field, the focal point \mathbf{x}_A subsequently acts as a virtual

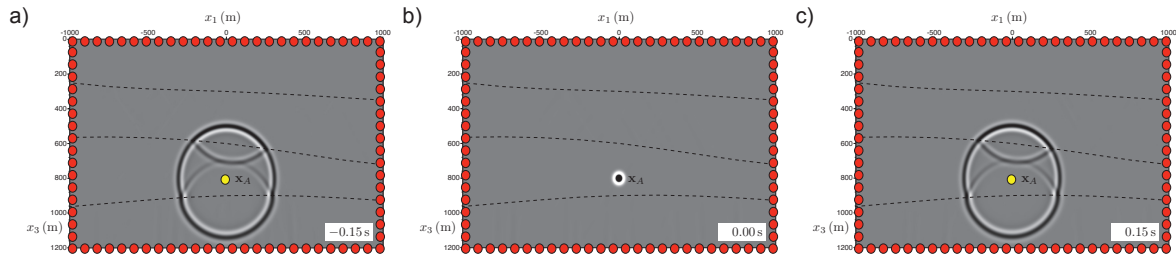


Figure 2 Illustration of the principle of time-reversal acoustics. According to the right-hand side of equation (1), a time-reversed field $G(\mathbf{x}, \mathbf{x}_A, -t)$ is emitted by sources at a closed boundary (denoted by the red dots) into an inhomogeneous medium. Panels (a), (b) and (c) show snapshots for $t = -0.15s$, $t = 0s$ and $t = +0.15s$, for fixed \mathbf{x}_A (the yellow dot) and variable \mathbf{x}_B . According to the left-hand side of equation (1), these snapshots represent the homogeneous Green's function $G_h(\mathbf{x}_B, \mathbf{x}_A, t) = G(\mathbf{x}_B, \mathbf{x}_A, t) + G(\mathbf{x}_B, \mathbf{x}_A, -t)$.

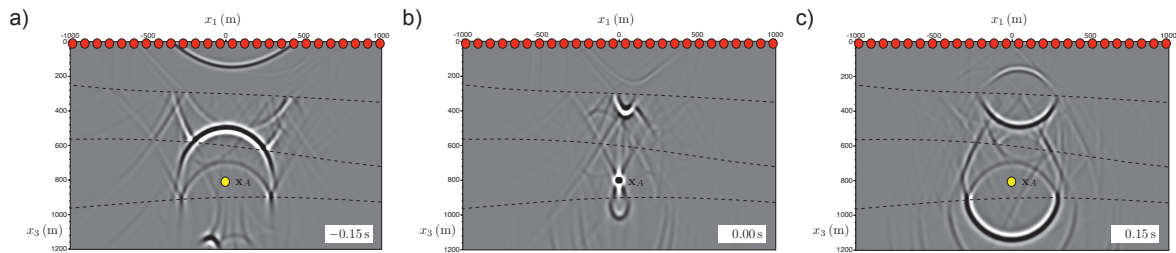


Figure 3 As in Figure 2, except this time the time-reversed field $G(\mathbf{x}, \mathbf{x}_A, -t)$ is emitted by sources from the upper boundary only (denoted by the red dots). Note that the snapshots no longer accurately represent the homogeneous Green's function $G_h(\mathbf{x}_B, \mathbf{x}_A, t)$.

source, which, for positive time, emits an exact replica of $G(\mathbf{x}, \mathbf{x}_A, t)$ into the inhomogeneous medium. Mathematically this is formulated as

$$G(\mathbf{x}_B, \mathbf{x}_A, t) + G(\mathbf{x}_B, \mathbf{x}_A, -t) \propto \oint_{\mathbb{S}} \underbrace{G(\mathbf{x}_B, \mathbf{x}, t)}_{\text{"propagator"}} * \underbrace{G(\mathbf{x}, \mathbf{x}_A, -t)}_{\text{"source"}} d\mathbf{x}, \quad (1)$$

where $*$ denotes convolution, \propto "proportional to", and \mathbb{S} represents the closed boundary. The right-hand side quantifies the emission of the time-reversed field from sources at \mathbf{x} at the boundary \mathbb{S} to any point \mathbf{x}_B inside the medium. The left-hand side shows the back-propagating field $G(\mathbf{x}_B, \mathbf{x}_A, -t)$ for negative time and the "virtual-source response" $G(\mathbf{x}_B, \mathbf{x}_A, t)$ for positive time. The superposition of these two functions is called the homogeneous Green's function $G_h(\mathbf{x}_B, \mathbf{x}_A, t)$, with

$$G_h(\mathbf{x}_B, \mathbf{x}_A, t) = G(\mathbf{x}_B, \mathbf{x}_A, t) + G(\mathbf{x}_B, \mathbf{x}_A, -t). \quad (2)$$

Equation (1) is an intuitive and somewhat simplified version of a more formal representation of the homogeneous Green's function (Porter, 1970; Oristaglio, 1989). Due to the time-reversal invariance of the wave equation, this representation holds for arbitrary inhomogeneous media. This implies it accounts for multiple scattering, which is illustrated in Figure 2. A serious practical drawback is the underlying assumption that the time-reversed field can be emitted into the medium from a closed boundary. In many situations, like in seismic exploration, the medium is accessible from one side only. Hence, for practical reasons one would have to replace the closed boundary \mathbb{S} in equation (1), by an open boundary \mathbb{S}_0 , representing the earth's surface. In that case equation (1) no longer holds, as is illustrated in Figure 3. Hence, for practical situations another approach is needed.

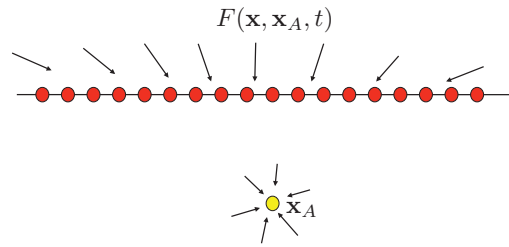


Figure 4 Configuration for the single-sided homogeneous Green's function representation. A focusing function $F(\mathbf{x}, \mathbf{x}_A, t)$ is emitted from the accessible boundary into the inhomogeneous medium.

A single-sided homogeneous Green's function representation

For the situation that the inhomogeneous medium is accessible from one side only, we derived the following single-sided representation of the homogeneous Green's function (Wapenaar et al., 2017)

$$G(\mathbf{x}_B, \mathbf{x}_A, t) + G(\mathbf{x}_B, \mathbf{x}_A, -t) = \int_{\mathbb{S}_0} G(\mathbf{x}_B, \mathbf{x}, t) * F(\mathbf{x}, \mathbf{x}_A, t) d\mathbf{x} + \int_{\mathbb{S}_0} G(\mathbf{x}_B, \mathbf{x}, -t) * F(\mathbf{x}, \mathbf{x}_A, -t) d\mathbf{x}, \quad (3)$$

with

$$\partial_t F(\mathbf{x}, \mathbf{x}_A, t) = -\frac{2}{\rho(\mathbf{x})} \partial_3 (f_1^+(\mathbf{x}, \mathbf{x}_A, t) - f_1^-(\mathbf{x}, \mathbf{x}_A, -t)). \quad (4)$$

Here $f_1^+(\mathbf{x}, \mathbf{x}_A, t)$ and $f_1^-(\mathbf{x}, \mathbf{x}_A, t)$ are ‘‘Marchenko-type’’ focusing functions. These can be retrieved from the reflection response $R(\mathbf{x}', \mathbf{x}, t)$ at \mathbb{S}_0 and an estimate of the direct arrivals between \mathbb{S}_0 and the focal point \mathbf{x}_A (Slob et al., 2014; Wapenaar et al., 2014). The first integral on the right-hand side of equation (3) has a similar form as the integral in equation (1), except that the time-reversed Green's function $G(\mathbf{x}, \mathbf{x}_A, -t)$ has been replaced by the focusing function $F(\mathbf{x}, \mathbf{x}_A, t)$ and the closed boundary \mathbb{S} has been replaced by the open boundary \mathbb{S}_0 . Hence, this first integral represents the emission of the focusing function from \mathbb{S}_0 into the medium (Figure 4). This is illustrated in Figure 5. According to the right-hand side of equation (3), the first integral and its time-reversal should be superposed. This is illustrated in Figure 6. The result is again the homogeneous Green's function $G_h(\mathbf{x}_B, \mathbf{x}_A, t) = G(\mathbf{x}_B, \mathbf{x}_A, t) + G(\mathbf{x}_B, \mathbf{x}_A, -t)$. Although this time it has been obtained from a single-boundary representation, it properly accounts for multiple scattering, similar as the result from the closed-boundary representation, shown in Figure 2.

Discussion

The single-sided representation of the homogeneous Green's function, as formulated in equation (3), has several interesting applications. First of all, note that the Green's function $G(\mathbf{x}_B, \mathbf{x}, t)$ on the right-hand side can be obtained from a similar representation. To see this, replace in the right-hand side of equation (3) \mathbb{S}_0 by \mathbb{S}'_0 just above \mathbb{S}_0 , replace \mathbf{x} on \mathbb{S}_0 by \mathbf{x}' on \mathbb{S}'_0 , \mathbf{x}_B inside the medium by \mathbf{x} on \mathbb{S}_0 and \mathbf{x}_A by \mathbf{x}_B . This gives a representation for $G(\mathbf{x}, \mathbf{x}_B, t) + G(\mathbf{x}, \mathbf{x}_B, -t)$. Using source-receiver reciprocity we get

$$G(\mathbf{x}_B, \mathbf{x}, t) + G(\mathbf{x}_B, \mathbf{x}, -t) = \int_{\mathbb{S}'_0} G(\mathbf{x}', \mathbf{x}, t) * F(\mathbf{x}', \mathbf{x}_B, t) d\mathbf{x}' + \int_{\mathbb{S}'_0} G(\mathbf{x}', \mathbf{x}, -t) * F(\mathbf{x}', \mathbf{x}_B, -t) d\mathbf{x}'. \quad (5)$$

Note that $G(\mathbf{x}', \mathbf{x}, t)$, with \mathbf{x} and \mathbf{x}' both at the surface, represents reflection data at the surface. Equation (5) redatums the receivers from \mathbf{x}' at the surface to \mathbf{x}_B in the subsurface. Next, after substituting the result into equation (3), the sources are redatumed from \mathbf{x} at the surface to \mathbf{x}_A in the subsurface. This two-step procedure brings sources and receivers from the surface to arbitrary virtual-source and virtual-receiver positions in the subsurface. For weakly scattering media (ignoring multiples), this method is akin to prestack source-receiver redatuming (Berkhout, 1982; Berryhill, 1984). For strongly scattering media (including multiple scattering) a similar two-step process, called source-receiver interferometry, has previously been formulated in terms of closed-boundary representations for the homogeneous Green's function (Halliday and Curtis, 2010). Our method replaces the closed boundary representations in the latter method by single-sided representations. Once $G(\mathbf{x}_B, \mathbf{x}_A, t) + G(\mathbf{x}_B, \mathbf{x}_A, -t)$ is obtained, a multiple-free image can be formed by setting \mathbf{x}_B equal to \mathbf{x}_A and taking $t = 0$. However, $G(\mathbf{x}_B, \mathbf{x}_A, t) + G(\mathbf{x}_B, \mathbf{x}_A, -t)$

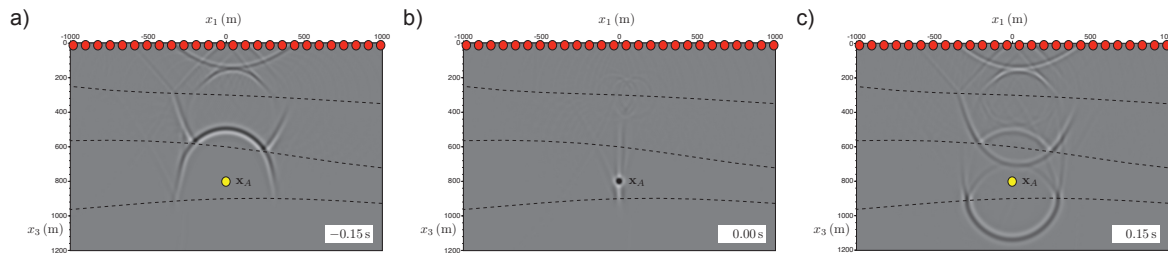


Figure 5 Illustration of the single-sided representation. According to the first term on the right-hand side of equation (3), a focusing function $F(\mathbf{x}, \mathbf{x}_A, t)$ is emitted by sources at a single boundary (denoted by the red dots) into an inhomogeneous medium. Panels (a), (b) and (c) show snapshots for $t = -0.15s$, $t = 0s$ and $t = +0.15s$, for fixed \mathbf{x}_A (the yellow dot) and variable \mathbf{x}_B .

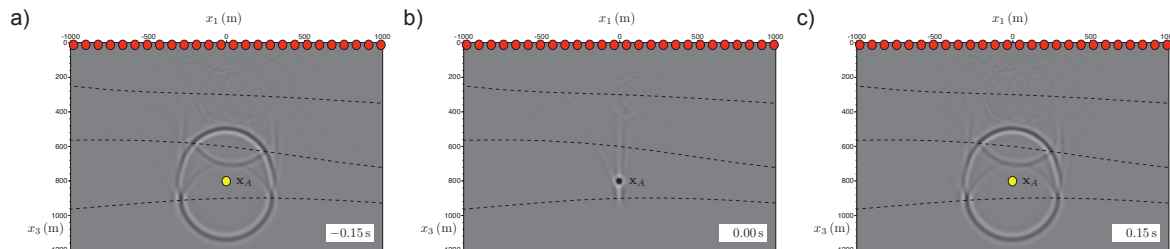


Figure 6 Illustration of the single-sided representation (continued). According to the right-hand side of equation (3), the results of Figure 5 should be reversed in time and added to its original. In other words, panels (c), (b) and (a) should be added to panels (a), (b) and (c), respectively. This yields panels (a), (b) and (c) of the current figure. According to the left-hand side of equation (3), these snapshots represent again the homogeneous Green's function $G_h(\mathbf{x}_B, \mathbf{x}_A, t) = G(\mathbf{x}_B, \mathbf{x}_A, t) + G(\mathbf{x}_B, \mathbf{x}_A, -t)$.

for variable and independent virtual sources and virtual receivers contains a wealth of additional information about the interior of the medium. This information can be used to assess for example AVA effects. However, the single-sided representation also opens the way to entirely different applications, such as the analysis of induced seismic responses and the forecasting of the complex propagation and scattering of the wavefield from potential future induced earthquakes.

References

- Berkhout, A.J. [1982] *Seismic Migration. Imaging of acoustic energy by wave field extrapolation. A. Theoretical aspects*. Elsevier.
- Berryhill, J.R. [1984] Wave-equation datuming before stack. *Geophysics*, **49**, 2064–2066.
- Esmersoy, C. and Oristaglio, M. [1988] Reverse-time wave-field extrapolation, imaging, and inversion. *Geophysics*, **53**, 920–931.
- Fink, M. [1997] Time reversed acoustics. *Physics Today*, **50**, 34–40.
- Halliday, D. and Curtis, A. [2010] An interferometric theory of source-receiver scattering and imaging. *Geophysics*, **75**(6), SA95–SA103.
- Oristaglio, M.L. [1989] An inverse scattering formula that uses all the data. *Inverse Problems*, **5**, 1097–1105.
- Porter, R.P. [1970] Diffraction-limited, scalar image formation with holograms of arbitrary shape. *Journal of the Optical Society of America*, **60**, 1051–1059.
- Slob, E., Wapenaar, K., Brogini, F. and Snieder, R. [2014] Seismic reflector imaging using internal multiples with Marchenko-type equations. *Geophysics*, **79**(2), S63–S76.
- Wapenaar, K., Fokkema, J. and Snieder, R. [2005] Retrieving the Green's function in an open system by cross-correlation: a comparison of approaches (L). *Journal of the Acoustical Society of America*, **118**, 2783–2786.
- Wapenaar, K., Thorbecke, J., van der Neut, J., Brogini, F., Slob, E. and Snieder, R. [2014] Marchenko imaging. *Geophysics*, **79**(3), WA39–WA57.
- Wapenaar, K., Thorbecke, J., van der Neut, J., Slob, E. and Snieder, R. [2017] Review paper: Virtual sources and their responses, Part II: data-driven single-sided focusing. *Geophysical Prospecting*, **65**, 1430–1451.